ACADEMIC PRESS

Biochemical and Biophysical Research Communications 297 (2002) 1154–1158

BBRC

www.academicpress.com

Molecular model of cyclin-dependent kinase 5 complexed with roscovitine

Walter Filgueira de Azevedo Jr.,[a,b,*] Renato Tadeu Gaspar,[a] Fernanda Canduri,[a,b] João Carlos Camera Jr.,[a] and Nelson José Freitas da Silveira[a]

[a] *Departamento de Física, IBILCE, UNESP São José do Rio Preto, SP 15054-000, Brazil*
[b] *Center for Applied Toxinology, Instituto Butantan, Av. Vital Brasil 1500, São Paulo, SP 05503-900, Brazil*

Received 19 August 2002

Abstract

Here is described a structural model for the binary complex CDK5–roscovitine. Roscovitine has been shown to potently inhibit cyclin-dependent kinases 1, 2 and 5 (CDK1, 2, and 5), and the structure of CDK2 complexed with roscovitine has been reported; however, no structural data are available for complexes of CDK5 with inhibitors. The structural model indicates that roscovitine strongly binds to the ATP-binding pocket of CDK5 and structural comparison of the CDK2–roscovitine complex correlates the structural differences with differences in inhibition of these CDKs by this inhibitor. This structure opens the possibility of testing new inhibitor families, in addition to new substituents for the already known lead structures of adenine derivatives.

Keywords: CDK; Roscovitine; Bioinformatics; Structure; Drug design

Cyclin-dependent kinases (CDKs) control the progression of cell cycle [1,2]. CDKs are constituted of a catalytic subunit and a regulatory subunit (cyclin) [3]. Each step of the cell cycle is thought to be regulated by such CDK–cyclin complexes. However, certain CDKs do not participate in controlling cell cycle, but they are rather involved in controlling cell differentiation in neuronal and muscle cells [4,5]. In addition, CDK also play a role in apoptosis (CDK2) and in the control of transcription (CDKs7, 8, 9) [6,7].

CDK5 is a unique member of the CDK family of kinases. Although the CDK5 is widely expressed in many tissues and cells, CDK5 kinase activity is restricted to neuronal cells [8]. This specificity for neuronal tissue is the result of the CDK5 activator proteins p35, p25, and p39. CDK5 is a multifunctional kinase that associates with other cell proteins to interact with the cytoskeleton and form supramolecular complexes. Recent investigations have revealed that most of the CDK5 in cells forms large multimeric complexes of high molecular weight, ranging from 60 to 670 kDa, in which CDK5 is associated with p25, p35, synapsin, τ-, β-catenins, and *N*-cadherins [4]. Increased CDK5 kinase activity has been implicated in Alzheimer's disease. Furthermore, pretreatment of cells with CDK5 inhibitors protected cells against neuronal death [9]. Since deregulation of CDK5 has been implicated in Alzheimer's disease, there is strong interest in chemical inhibitors of CDK5 that could play an important role in the discovery of anti-Alzheimer's disease agents.

Roscovitine [2-(*R*)-(1-ethyl-2-hydroxy-ethylamino)-6-benzylamino-9-isopropylpurine] is a purine analog that has been shown to potently inhibit CDK, with IC50 values ranging from 0.16 μM (for CDK5) to over 100 μM (for CDK4 and CDK6) [10]. The crystallographic structure of the binary complex of CDK2–roscovitine indicates that the inhibitor is strongly bound in the ATP-binding pocket of CDK2. This article describes the modeling of human CDK5 complexed with roscovitine. The investigation was made in order to gain further insight into the structural basis for chemical inhibition of CDK5.

* Corresponding author. Fax: +55-17-221-2247.
E-mail address: walterfa@df.ibilce.unesp.br (W.F. de Azevedo Jr.).

0006-291X/02/$ - see front matter © 2002 Elsevier Science (USA). All rights reserved.
PII: S0006-291X(02)02352-5

Methods

Molecular modeling. The structure of CDK5 complexed with p25 has been recently determined [11] and a molecular model for CDK5 complexed with the peptide PKTPKKAKKL has also been reported [12]; however, the atomic coordinates for CDK5 are not available. Therefore, for modeling of the CDK5 we used a protocol previously described for modeling of CDK9 [13]. In brief, model building of CDK5 was carried out using the program MODELLER [14]. The atomic coordinates of eight crystallographic CDK2 structures solved to resolution better than 2.1 Å were used to build up an ensemble of CDK2 structures to be used as starting models for modeling of the CDK5. The alignment of CDK2 (template) and CDK5 (target) is shown in Fig. 1. Next, the spatial restraints and CHARMM energy terms enforcing proper stereochemistry [15] were combined into an objective function. Finally, the model is obtained by optimizing the objective function in Cartesian space. The optimization is carried out by the use of the variable target function method [16] employing methods of conjugate gradients and molecular dynamics with simulated annealing. Several slightly different models can be calculated by varying the initial structure. We generated 500 CDK5 models and the final model was selected based on stereochemical quality. The roscovitine molecule from the CDK2–roscovitine structure was superposed onto the best CDK5 model. Further optimization of the complex CDK5–roscovitine was performed following the procedure described for CDK5 model. All optimization process was performed on SGI Octane, R12000.

Analysis of the model. The overall stereochemical quality of the final model for CDK5 was assessed by the program PROCHECK [17]. Atomic models were superposed using the program LSQKAB from CCP4 [18]. The cutoff for hydrogen bonds and salt bridges was 3.6 Å. The contact surfaces for the binary complexes were calculated using AREAIMOL and RESAREA [18].

Results and discussion

Quality of the model

Fig. 2 shows the Ramachandran diagram ϕ–ψ plots for the binary complex of CDK5–roscovitine. The Ramachandran plot for the eight CDK2 structures was also generated (figure not shown) to compare the overall stereochemical quality of CDK5 model against CDK2 structures solved by biocrystallography. Analysis of the Ramachandran plot of the best CDK5 model shows that 91.0% of the residues lies in the most favorable regions, 8.2% in the additional allowed regions, and 0.8% in the disallowed regions (Asp97 and Ala198). The same analysis for eight crystallographic CDK2 structures presents 89.8% of residues in the most favorable, 9.7% in additional allowed regions, and 0.5% in generously allowed regions. The overall rating for the model is better than the one obtained for the eight structures of CDK2.

Overall description

The model of the kinase in the complex CDK5–roscovitine is folded into the typical bilobal structure as was observed for CDK2 structure [19,20], with the smaller N-terminal lobe consisting predominantly of β-sheet structure and the larger C-terminal lobe consisting primarily of α-helices. Fig. 3 shows a schematic drawing of the complex CDK5–roscovitine. The N-terminal lobe of CDK5 consists of a sheet of five antiparallel β-strands (β1–β5) and a single large helix (α1). The C-terminal lobe contains a pseudo-4-helical bundle (α2, 3, 4, 6), a small β-ribbon (β6–β8), and two additional helices (α5, 7). The roscovitine molecule is found in the cleft between the two lobes.

Molecular fork

Analysis of the many available crystal structures of CDK2–inhibitor complexes reveals the existence of conserved interactions that appear to be determinant for recognition of the small molecules by the ATP-binding pocket of this class of enzymes. The participation of a molecular fork composed of C═O group on Glu81, N–H group, and C═O group in Leu83 in hydrogen bonds between CDK2 and inhibitor has been observed on several CDK2–inhibitor structures. Furthermore, the molecular model for CDK9 complexed with flavopiridol also presented the molecular fork [13]. In the CDK5–roscovitine model this molecular fork is composed of C═O on Glu81, N–H, and C═O on Cys83 and participates in hydrogen bonds between CDK5 and roscovitine.

Side chain positions

To find out whether roscovitine binding to CDK5 induces changes in side chain conformation in the binding pocket, we compared the binding pockets of CDK5 complexed with roscovitine and CDK2 complexed with ATP (PDB access code: 1HCK) after a

```
                    15                  30                  45                  60                  75
CDK2 MENFQKVEKIGEGTYGVVYKARNKLTGEVVALKKIRLDTETEGVPSTAIREISLLKELNHPNIVKLLDVIHTENKLYLVFEFLHQDLKK 89
CDK5 MQKYEKLEKIGEGTYGTVFKAKNRETHEIVALKRVRLDDDDEGVPSSALREICLLKELKHKNIVRLHDVLHSDKKLTLVFEFCDQDLKK 89
     *    * ********* * ** *  * * ****  ***   ***** * *** ***** * * * * ** *   ** *****  *****

     90                  105                 120                 135                 150                 165
CDK2 FMDASALTGIPLPLIKSYLFQLLQGLAFCHSHRVLHRDLKPQNLLINTEGAIKLADFGLARAFGVPVRTYTHEVVTLWYRAPEILLGCK 178
CDK5 YFD-SCNGDLDPEIVKSFLFQLLKGLGFCHSRNVLHRDLKPQNLLINRNGELKLADFGLARAFGIPVRCYSAEVVTLWYRPPDVLFGAK 177
       * *           ** ***** ** ****  **************  *  ************ *** *  ******** *  * * *

     180                 195                 210                 225                 240                 255
CDK2 YYSTAVDIWSLGCIFAEMVTR-RALFPGDSEIDQLFRIFRTLGTPDEVVWPGVTSMPDYKPSFPKWARQDFSKVVPPLDEDGRSLLSQM 267
CDK5 LYSTSIDMWSAGCIFAELANAGRPLFPGNDVDDQLKRIFRLLGTPTEEQWPSMTKLPDYKPYPMYPATTSLVNVVPKLNATGRDLLQNL 266
      ***  * ** ******     * ****    *** **** **** *  **  *  *****     *      *** *   ** **

      270                 285
CDK2 LHYDPNKRISAKAALAHPFFQDVTKPVPHLRL  297
CDK5 LKCNPVQRISAEEALQHPYFSDFCPP------  298
     *   *  ****  ** ** * *   *
```

Fig. 1. Sequence alignment of human CDK2 and CDK5. There is 40.4% identity between CDK2 and CDK5 sequences in the modelled region. The alignment was performed with the program CLUSTAL V [25].

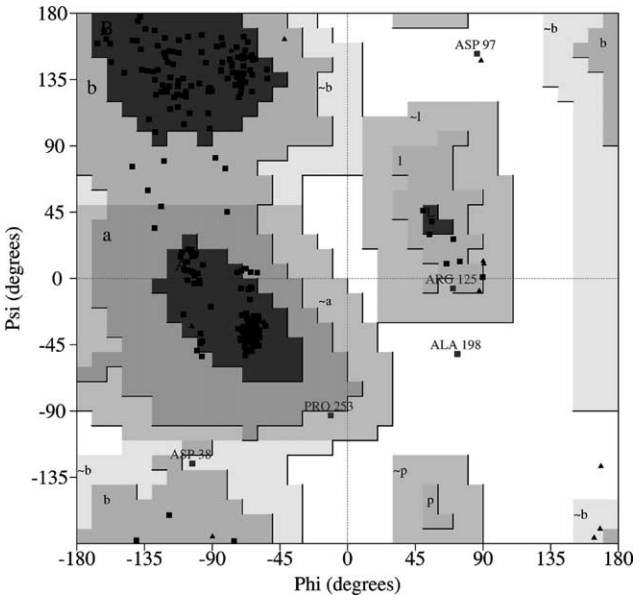

Fig. 2. Ramachandran plot for the CDK5. The regions A, B, and L are more favorable, the regions a, b, l, and p are allowed and ~a, ~b, ~l, and ~p are generously allowed regions. Glycine residues are shown as triangles.

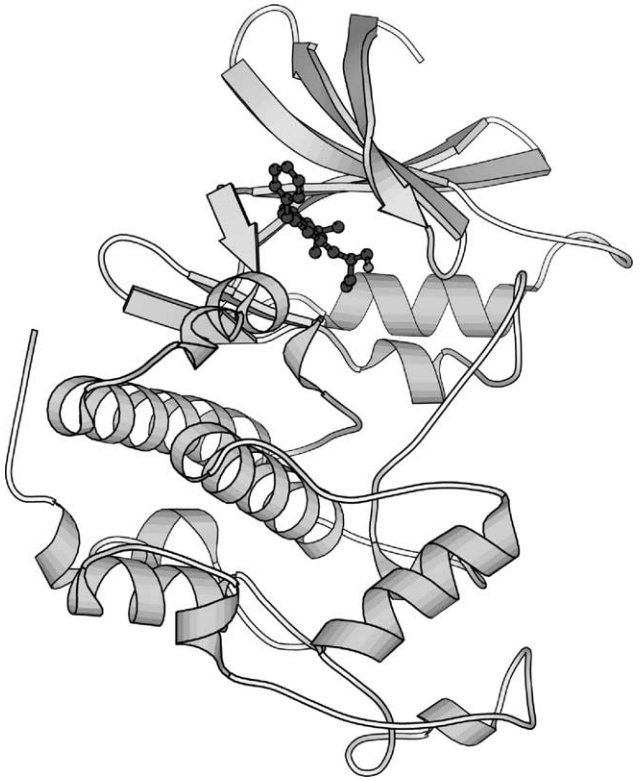

Fig. 3. Ribbon diagram of the human CDK5 generated by Molscript [26].

superposition of the models based on their Cα atoms. This superposition revealed the significant movement of two side chains. For the roscovitine complex, it was observed that Lys20 changed its position, with NZ moving by 1.97 Å away from its position in the ATP complex and Phe82 changed its position, with CZ moving by 2.91 Å away from its position in the ATP complex. No significant movements were observed on the side chains in the ATP-binding pocket of the complex CDK5–roscovitine. In summary, roscovitine fits very well to the binding pocket with small adjustments in the side chains.

Interactions of roscovitine with CDK5

The specificity and affinity between enzyme and its inhibitor depend on directional hydrogen bonds and ionic interactions, as well as on shape complementarity of the contact surfaces of both partners [21–23]. A total of five hydrogen bonds were observed between CDK5 and roscovitine, in binary model, involving the residues Cys83, Asp86, and Gln130. For the CDK2–roscovitine model two hydrogen bonds involving the residue Leu83 were observed. Table 1 shows the intermolecular hydrogen bonds for both complexes. The higher number of intermolecular hydrogen bonds, observed in the CDK5–roscovitine complex, is probably due to the modification of His84 (CDK2) to Asp in the CDK5 sequence, which allows an additional salt bridge in the CDK5 structure, involving Asp84 and Lys20. This salt bridge moves the inhibitor away from the molecular fork of CDK5, however, keeping the intermolecular hydrogen bonds between the molecular fork and roscovitine. Nevertheless, this movement is enough to bring roscovitine closer to the side chains of Gln130 and Asp86, which allows additional intermolecular hydrogen bonds.

Superposition of the CDK2–ATP onto CDK5–roscovitine structure indicates that the two ring systems of roscovitine and ATP overlap approximately in the same plane, however, with different orientations. As observed for the crystallographic structure of roscovitine bound to CDK2 [3], the region of CDK5 occupied by the phenyl ring of roscovitine is pointing away from the ATP-binding pocket and partially exposed to solvent. Fig. 4 shows the ATP-binding pocket for the complexes CDK2–ATP and CDK5–roscovitine.

The electrostatic potential surface of the CDK2–roscovitine and the model of CDK5 complexed with the same inhibitor were calculated with GRASP [24]. The analysis of the charge distribution of the binding pockets indicates the presence of some charge comple-

Table 1
Intermolecular hydrogen bonds between CDK5 and roscovitine

Roscovitine	CDK	Residue, atom	Distance (Å)
N6	CDK2	Leu83 O	2.82
N7	CDK2	Leu83 N	3.38
N6	CDK5	Cys83 O	3.10
N7	CDK5	Cys83 N	3.53
O1	CDK5	Gln130 NE2	3.29
N2	CDK5	Asp86 OD2	3.54
N1	CDK5	Asp86 OD2	3.16

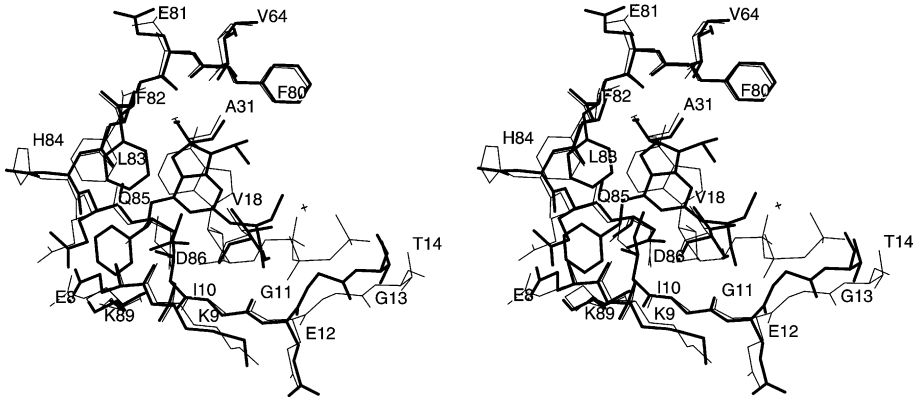

Fig. 4. Superimposed binding pockets of CDK5–roscovitine complex (thick line) and CDK2–ATP complex (thin line).

mentarity between inhibitor and enzyme; nevertheless, most of the binding pocket is hydrophobic in both structures.

Conclusions

The overall structure of the complex indicates that the roscovitine is tightly bound to the ATP-binding pocket and no further ATP-binding sites were identified in the CDK5 structure. Both complexes presented the same contact areas (334 $\AA^2$), with no direct correlation with the activity of these inhibitors. This is probably because they are all very specific inhibitors for CDK2 and CDK5. Analysis of the number of hydrogen bonds between roscovitine and CDK5 and CDK2 shows that the CDK5–roscovitine complex has a higher number of intermolecular hydrogen bonds, which indicates that roscovitine has higher affinity for CDK5 than for CDK2. The IC50 values for inhibition by roscovitine of CDK2 and CDK5 are 0.70 and 0.16 μM, respectively [10].

The analysis of the structural models and activity experiments strongly indicates that the comparison of structures of different enzymes complexed with same inhibitor (roscovitine complexed with CDK5 and CDK2) can be used for a qualitative analysis of the activity of these inhibitors against different enzymes. Furthermore, the molecular fork identified in CDK2 structures and CDK9 molecular model seems to be conserved in CDK5 structure, and also participates in hydrogen bonds with inhibitors, which suggests that CDK5 may also be strongly inhibited by other CDK2 inhibitors, which opens the possibility of testing new inhibitors. Further inhibition experiments may confirm this prediction.

Acknowledgments

We thank Andressa Salbé dos Santos Oliveira for English revision. This work was supported by grants from FAPESP (SMOLBNet), CNPq, CAPES, and Fundo Bunka de Pesquisa (Banco Sumitomo). W.F.A. Jr. is a researcher for the Brazilian Council for Scientific and Technological Development (CNPq, 300851/98-7).

References

[1] C. Norbury, P. Nurse, Animal cell cycles and their control, Annu. Rev. Biochem. 61 (1992) 441–470.
[2] W.F. de Azevedo Jr., H.J. Mueller-Dieckmann, U. Schulze-Gahmen, P.J. Worland, E. Sausville, S.-H. Kim, Structural basis for specificity and potency of a flavonoid inhibitor of human CDK2, a cell cycle kinase, Proc. Natl. Acad. Sci. USA 93 (7) (1996) 2735–2740.
[3] W.F. de Azevedo Jr., S. Leclerc, L. Meijer, L. Havlicek, M. Strnad, S.-H. Kim, Inhibition of cyclin-dependent kinases by purine analogues: crystal structure of human CDK2 complexed with roscovitine, Eur. J. Biochem. 243 (1997) 518–526.
[4] G.N. Patrick, L. Zuckerberg, M. Nikolic, S. de la Monte, P. Dikkes, L.H. Tsai, Conversion of p35 to p25 deregulates Cdk5 activity and promotes neurodegeneration, Nature 402 (6762) (1999) 615–622.
[5] R.B. Maccioni, C. Otth, I.I. Concha, J.P. Muñoz, The protein kinase Cdk5. Structural aspects, roles in neurogenesis and involvement in Alzheimer's pathology, Eur. J. Biochem. 268 (6) (2001) 1518–1527.
[6] S.H. Chao, K. Fujinaga, J.E. Marion, R. Taube, E.A. Sausville, A.M. Senderowicz, B.M. Peterlin, D.H.J. Price, Flavopiridol inhibits P-TEFb and blocks HIV-1 replication, J. Biol. Chem. 275 (37) (2000) 28345–28348.
[7] N. Gray, L. Detivaud, C. Doerig, L.C. Meijer, ATP-site directed inhibitors of cyclin-dependent kinases, Curr. Med. Chem. 6 (9) (1999) 859–875.
[8] P.M. Clare, R.A. Poorman, L.C. Kelley, K.D. Watenpaugh, C.A. Bannow, K.L. Leach, The cyclin-dependent kinases CDK2 and CDK5 act by a random, anticooperative kinetic mechanism, J. Biol. Chem. 276 (51) (2001) 48292–48299.
[9] A. Alvarez, R. Toro, A. Cárceres, R.B. Maccioni, Inhibition of tau phosphorylating protein kinase CDK5 prevents β-amyloid-induced neuronal death, FEBS Lett. 459 (3) (1999) 421–426.
[10] L. Meijer, A. Borgne, O. Mulner, J.P. Chong, J.J. Blow, N. Inagaki, Biochemical and cellular effects of roscovitine, a patent and selective inhibitor of the cyclin-dependent kinases CDK2 and CDK5, Eur. J. Biochem. 243 (1997) 527–536.
[11] C. Tarricone, R. Dhavan, J. Peng, L.B. Areces, L.H. Tsai, A. Musacchio, Structure and regulation of the CDK5–p25(nck5a) complex, Mol. Cell 8 (3) (2001) 657–669.
[12] P. Sharma, P.J. Steinbach, M. Sharma, N.D. Amin, J.J. Barchi Jr., H.C. Pant, Identification of substrate binding site of cyclin-dependent kinase 5, J. Biol. Chem. 274 (1999) 9600–9606.

[13] W.F. de Azevedo Jr., F. Canduri, N.J.F. da Silveira, Structural basis for inhibition of cyclin-dependent kinase 9 by flavopiridol, Biochem. Biophys. Res. Commun. 293 (2002) 566–571.
[14] A. Sali, T.L. Blundell, Comparative protein modelling by satisfaction of spatial restraints, J. Mol. Biol. 234 (1993) 779–815.
[15] B.R. Brooks, R.E. Bruccoleri, B.D. Olafson, D.J. States, S. Swaminathan, M. Karplus, CHARMM: a program for macromolecular energy minimization and dynamics calculations, J. Comp. Chem. 4 (1983) 187–217.
[16] W. Braun, N. Go, Calculation of protein conformations by proton–proton distance constraints. A new efficient algorithm, J. Mol. Biol. 186 (3) (1985) 611–626.
[17] R.A. Laskowski, M.W. MacArthur, D.K. Smith, D.T. Jones, E.G. Hutchinson, A.L. Morris, D. Naylor, D.S. Moss, J.M. Thorton, PROCHECK v.3.0—program to check the stereochemistry quality of protein structures—operating instructions, 1994.
[18] Collaborative Computational Project No. 4. The CCP4 Suite: programs for protein crystallography, Acta Crystallogr. D 50 (1994) 760–763.
[19] H.L. DeBondt, J. Rosenblatt, J. Jancarik, H.D. Jones, D.O. Morgan, S.-H. Kim, Crystal structural of cyclin-dependent kinase 2, Nature (Lond.) 363 (1993) 595–602.
[20] S. Serota, E. Radsio-Andzelm, Three protein kinase structures define a common motif, Structure 2 (1994) 345–355.
[21] F. Canduri, L.G.V.L. Teodoro, C.C.B. Lorenzi, V. Hial, R.A.S. Gomes, J. Ruggiero Neto, W.F. de Azevedo Jr., Crystal structure of human uropepsin at 2.45 Å resolution, Acta Crystallogr. D 57 (2001) 1560–1570.
[22] W.F. de Azevedo Jr., F. Canduri, V. Fadel, L.G.V.L. Teodoro, V. Hial, R.A.S. Gomes, Molecular model for the binary complex of uropepsin and pepstatin, Biochem. Biophys. Res. Commun. 287 (1) (2001) 277–281.
[23] S.-H. Kim, U. Schulze-Gahmen, J. Brandsen, W.F. de Azevedo Jr., Structural basis for chemical inhibitor of CDK2, Prog. Cell Cycle Res. 2 (1996) 137–145.
[24] A. Nicholls, K.A. Sharp, B. Honig, Protein folding and association: insights from the interfacial and thermodynamic properties of hydrocarbons, Proteins 11 (4) (1991) 281–296.
[25] D.G. Higgins, A.J. Bleasby, R. Fuchs, CLUSTAL V: Improved software for multiple sequence alignment, Comput. Appl. Biosci. 8 (2) (1992) 189–191.
[26] P. Kraulis, MOLSCRIPT: A program to produce both detailed and schematic plots of proteins, J. Appl. Cryst. 24 (1991) 946–950.